STRUCTURAL EVOLUTION OF STEEL-BASED MMC BY HIGH ENERGY X-RAY DIFFRACTION AND MICROMECHANICAL APPROACH

G. Geandier[1,2*], M. Dehmas[1,2], M. Mourot[1,2], E. Aeby Gautier[1,2], S. Denis[1,2], O. Martin[3], N. Karnatak[3]

[1] CNRS - Institut Jean Lamour - UMR CNRS 7198 – École des Mines de Nancy - Parc de Saurupt - CS 14234 - 54042 NANCY Cedex – France
[2] Université de Lorraine - Institut Jean Lamour - UMR CNRS 7198 – École des Mines de Nancy - Parc de Saurupt - CS 14234 - 54042 NANCY Cedex – France
[3] Mecachrome, 27 rue de la Milletière, 37073 Tours Cedex 2, France
**guillaume.geandier@ijl.nancy-universite.fr*

Keywords: metal matrix composite, X-ray diffraction, microstructure, finite element

Abstract
In situ high energy X-ray diffraction synchrotron was used to provide direct analysis of the transformation sequences in steel-based matrix composite (MMC) reinforced with TiC particles elaborated by powder metallurgy. Evolution of the phase fractions of the matrix and TiC particles as well as the mean cell parameters of each phase were determined by Rietveld refinement from high energy X-ray diffraction (ID15B, ESRF, Grenoble, France). Moreover some peaks were further analysed in order to obtain the X-Ray strain during the cooling step. Non-linear strain evolutions of each phase are evidenced that are either associated with differences in the coefficient of thermal expansion (CTE) between matrix and TiC particle or to the occurrence of phase transformation. Micromechanical calculations were performed by finite element method to estimate the stress state in each phase and outline the effects of differences in CTE and those of volume change associated with the matrix phase transformation. The calculated results led to a final compressive hydrostatic stress in the TiC reinforcement and tensile hydrostatic stress in the matrix area around the TiC particles. Moreover, the tendencies measured from in situ synchrotron diffraction (mean cell parameters) matched well with the numerical estimates.

1 Introduction

Steel-based metal matrix composites (MMC) reinforced by ceramic particles are developed to take the best part of the mechanical properties of both matrix and reinforcement. They combine a metallic matrix and reinforcement phase with final mechanical properties higher than the matrix itself [1]. Properties optimisation is correlated to the control of the MMC chemical composition, interface nature, origin of inconsistency and damage, of the matrix microstructure and by the stresses in the reinforced phase and the matrix [2-4].
In a previous study [5] on steel matrix composites elaborated by powder metallurgy and HIP'ed the authors outlined the role of the particles on the microstructure formation (kinetics and nature of the phases) as well as the development of stresses during thermal treatment of the composite. Indeed, stresses are generated during cooling either due to differences of CTE

and mechanical properties between the matrix and the reinforcement, [2, 3, 6, 7] or to volume change associated with phase transformations [8-10].
In this study, we further analyse the behaviour of the steel based MMC reinforced by TiC particles by in situ X-ray diffraction during thermal treatment that led to phase transformation in the matrix. From XRD patterns, we have extracted the phase fraction and the strain evolution in each phase during cooling. A clear influence of the phase transformation is revealed considering the strain evolution of each phase. In order to analyse the strain evolutions and the role of the transformation on the final mechanical state of the composite, a micromechanical model has been used to take into account each contribution to stress development: differences in CTE, mechanical properties and phase transformation.
In the following parts, we first describe the sample used for this study, then the experimental set-up for high energy X-ray diffraction. Results for XRD analysis are presented followed by the micromechanical model and its principal results.

2 Sample

Mecachrome elaborated steel-TiC composite. At first, mechanical milling of TiC particles and steel powders was performed at relatively low energy in order to reduce the size of both components. The consolidation of the composite powder was further realized by hot isostatic pressing (HIP) under a stress of 100 MPa at 1120°C during 4 hours. The chemical composition of the steel matrix was measured by glow discharge mass spectroscopy and summarized in table 1. The matrix contains 0.31 wt. % carbon but also 3.83 wt. % chromium and 0.72 wt. % molybdenum. For this composition a martensitic state is obtained after air cooling.

Fe	C	Cr	Mo	Mn	Si	Ni	V	N (ppm)
Bal.	0.31 ± 0.01	3.83 ± 0.02	0.72 ± 0.01	0.43 ± 0.01	0.59 ± 0.01	0.07 ± 0.01	0.12 ± 0.01	152 ± 16

table 1: chemical composition of the matrix (wt %)

3 Experimental methods

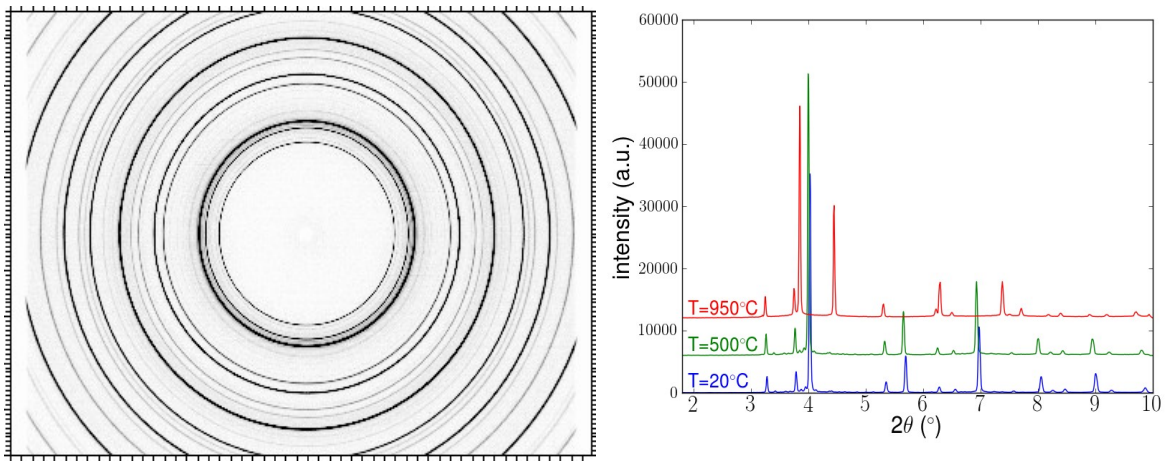

Figure 1: (left) XRD image from CCD detector at room temperature, (right) XRD diagrams after correction and reduction at different temperatures (intensity have been modified for clarity).

The X-ray diffraction (XRD) experiments were performed at the European Synchrotron Radiation Facility (ESRF, Grenoble, France), on the ID15B beam line. The in situ measurements were conducted by high energy X-ray synchrotron radiation diffraction at

various temperatures with a monochromatic beam of 89.12 keV. The high energy beam allowed to analyse a large volume of the sample, to be representative of the bulk behaviour and to minor the surface effect. Samples had a thickness of 3 mm in the beam direction. Beam size was fixed to 400x400µm^2. Samples were heated using a lamp furnace up to 960ºC and a thermocouple spot-welded on the sample surface allowed the measurement and control of the temperature. XRD patterns were recorded by flat CCD detector (pixium 4700), with one image every 3.5s (1s exposure + 2.5s readout time). A typical image is presented figure 1. Images were corrected and data reduced using fit2d software [11] to conventional XRD diagrams (2θ, intensity) that were analysed using Rietveld method [12] provided by Fullprof suite software [13]. The thermal treatment used was a heating at 0.5ºC/s to 1000ºC, a dwell for one hour and a cooling at 0.5ºC/s.

4 Results from in situ XRD analysis

XRD analysis was conducted for the whole thermal treatment. Only results on cooling are presented here. Mass fraction evolutions of each phase obtained from Rietveld analysis [12] are given in figure 2 versus temperature.

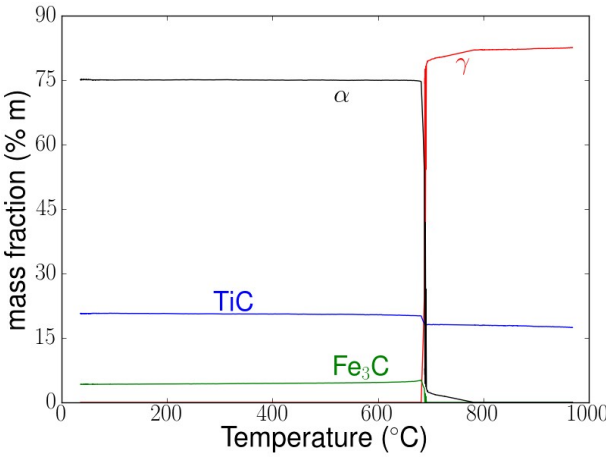

fiure 2: mass fraction evolution during cooling.

At the beginning of cooling, only austenite (γ) and TiC are present. Until 780°C only slight changes in the mass fractions of γ and TiC are observed. Ferrite (α) appears at 780ºC and formation of ferrite and cementite occurs between 690ºC and 670°C. In that temperature range, the TiC amount increases more clearly. Changes in TiC amounts are due to differences of carbon solubility in austenite and ferrite. The transformation kinetics of the matrix leads to a mixture of ferrite and pearlite. At temperatures lower than 670°C, the amount of all phases remains constant until room temperature.

Rietveld analysis allows extracting the mean cell parameters for each phase. Evolutions of the cell parameters are presented on figure 3a. Because the cell parameter evolutions are difficult to extract from Rietveld analysis to the small amount of phase present (<1%), X-ray strain analysis was performed on several peaks from each phases.

For the analysis, peak displacement was measured by fitting a single peak with a Pearson VII function. Strain was calculated by the equation (1).

$$\epsilon = \ln\left(\sin(\theta_0)/\sin(\theta)\right) \quad (1)$$

where θ and θ_0 are the peak position at a given temperature and at a reference point respectively. For austenite and TiC, reference was taken on the dwell at high temperature. For ferrite, it was fixed at the first point at which ferrite peak could be calculated correctly. Thus a direct comparison is only possible for austenite and TiC. However the slopes of the curves can be compared. The obtained results are presented in figure 3b.

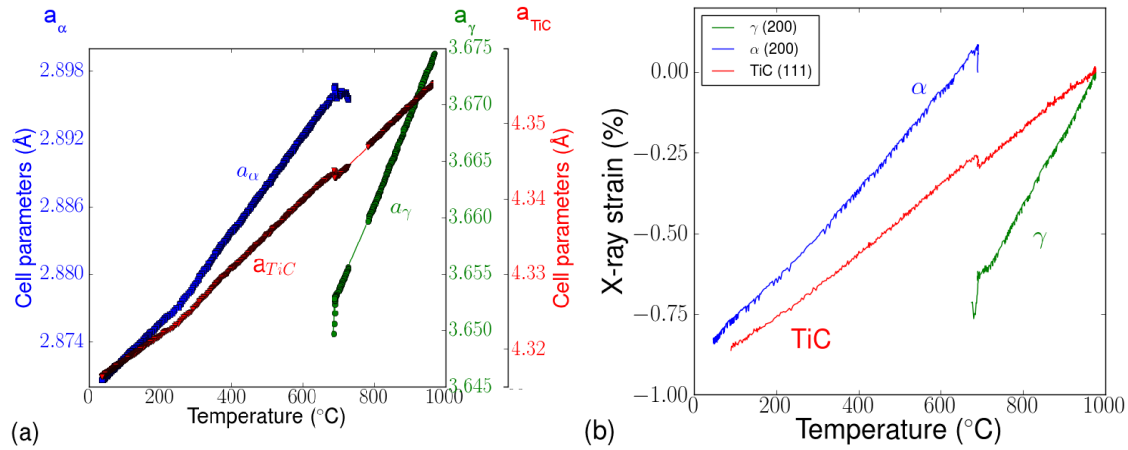

figure 3: mean cell parameters evolution during cooling and X-ray strain evolution during cooling on selected peaks.

From figure 3a and 3b, we can see that the evolutions of the cell parameter and strains are linear at the higher temperatures, when no phase transformation occurs. Between 780 and 690ºC, as a small amount of ferrite forms, strain in austenite is no more linear and the slope decreases. No change in the slope for TiC is observed. When ferrite-pearlite transformation occurs, we observe an abrupt change in the strain evolutions for the three phases (TiC, austenite and ferrite). Both TiC and ferrite present an increase of the X-Ray strain, while a decrease in the strain evolution is observed for austenite. These evolutions clearly show the generation of stresses during the phase transformation of the matrix that affects all phases in the composite.

When matrix transformation is fully completed, strain and cell parameters in each phase (TiC and ferrite) have a nearly linear evolution until 400ºC. From that temperature, slight deviations from linearity can be observed emphasizing some thermal stresses.

In order to further analyse the results observed during cooling a micro-mechanical model has been used to calculate the stress evolutions in each phase.

5 Finite element modeling

The MMC behaviour was calculated on cooling using a micro-mechanical model based on the F.E. Zebulon code [14]. For the actual model, only two "phases" were taken into account i) the reinforcement particle TiC, with an elastic behaviour and ii) the steel matrix with an elasto-visco-plastic behaviour. The behaviour law used for the matrix derivates from previous works on the experimental study on the mechanical behaviour during phase transformation and their modelling for the prediction of internal stresses in metallic alloys [8, 15-17]. It is dependent on temperature, the phase amount and the nature of the phase. For the present calculations properties were taken as those of austenite and ferrite. The behaviour law takes into account the phase transformation by imposing deformation due the volume variation between austenite and ferrite and transformation plasticity. So the total deformation will be described by equation (2) (in incremental form):

$$d\varepsilon_{ij}^{t} = d\varepsilon_{ij}^{e} + d\varepsilon_{ij}^{th} + d\varepsilon_{ij}^{tr} + d\varepsilon_{ij}^{vp} + d\varepsilon_{ij}^{tp} \qquad (2)$$

where exponent *t* represents the total deformation, *e* the elastic contribution, *th* the thermal contribution (by the coefficient of thermal expansion), *tr* the deformation due the volume variation associated with the transformation which is proportional to the transformation rate, *vp* the visco-plastic deformation and *tp* the transformation plasticity deformation proportional to the transformation rate and the local stress deviator.
The evolutions of the mechanical properties of the different phases versus temperature were extracted from literature for TiC [18] and previous studies on steels [17]. The CTE is equal to 8.1×10^{-6} K^{-1} for TiC 23.6×10^{-6} K^{-1} for austenite and 12.8×10^{-6} K^{-1} for ferrite.

For the calculation, in order to represent the composite, a 2D periodic distribution of round shape particles of TiC covering 20% of the whole surface is used. Figure 4 presents the unit cell and the finite element mesh. Symmetry and periodic conditions are imposed to the mesh. The 2D calculations were performed with a generalized plane strain condition. For the calculated results, evolutions are presented at three positions on the mesh, one in the centre of TiC particle, one in the matrix at the limit of the cell and one in the matrix close to the particle. The positions are noted TiC, limit and "interface" respectively on the figures.

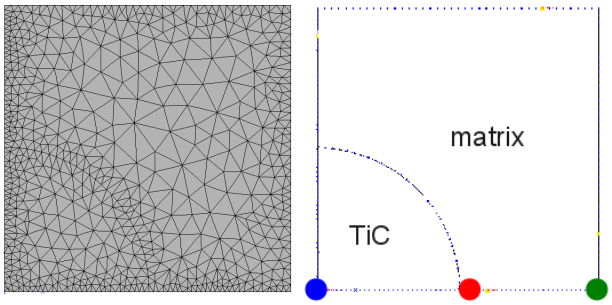

figure 4: mesh used for the micromechanical model composed of the spherical particle of TiC and square matrix.

The thermal treatment applied during the calculation is the cooling imposed during the XRD experiments, i.e. cooling rate of 0.5ºC/s. Phases are supposed to be fully relaxed at high temperature. Moreover, the transformation kinetics of the matrix is the one characterized by in situ XRD. TiC amount is supposed constant.

Figure 5 presents the evolution of the Von Mises stress and equivalent cumulated plastic deformation as a function of temperature at the different positions in the mesh. Figure 6 presents the evolution of the hydrostatic stress as a function of temperature for those different positions.
Between 1050°C and 780°C, the matrix is fully austenitic. Stresses are generated due to the large difference between the CTE of TiC and the matrix. Von Mises stress increases as temperature decreases both in TiC and the matrix, reaching values up to 200MPa in TiC and 100MPa in austenite. Moreover, due to the low yield stress of the matrix, plastic strains are generated with cumulated values reaching locally 0.4%. Considering the hydrostatic stress, TiC is in compression while the matrix is in tension at the limit of the mesh and in compression near the TiC particle.

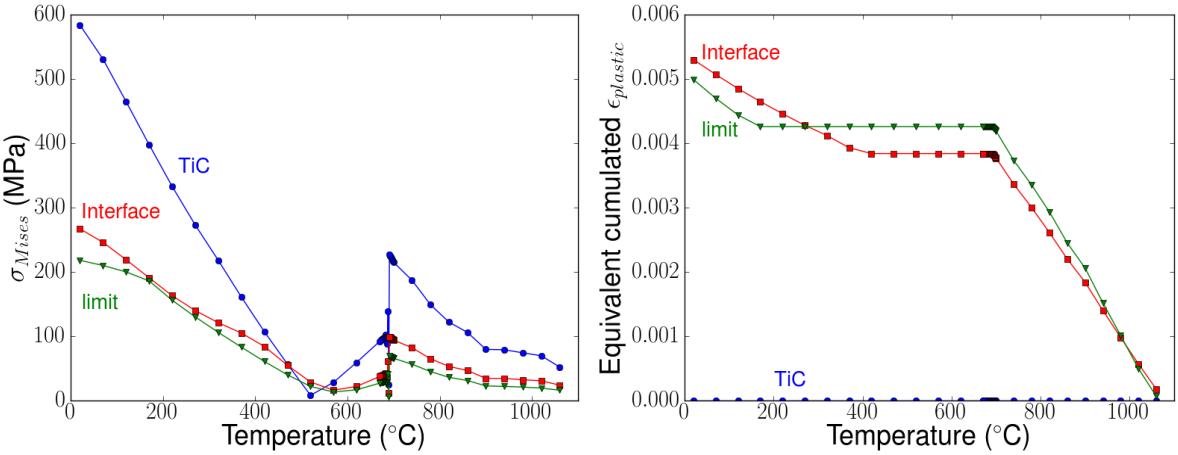

figure 5: Evolution of Von Mises stress and equivalent cumulated plastic strain versus temperature at different positions of the mesh.

When transformation begins, the small amount of ferrite formed between 780°C and 690ºC does not change the stress and cumulated strain evolutions. However, when transformation kinetics increases, i.e. between 690°C and 670°C, a sudden decrease of Von Mises stress is calculated in both TiC and the matrix, and whatever the location. For TiC particle, Von Mises stress decreases while hydrostatic stress varies from compression to tension. This evolution of the hydrostatic stress between 690°C and 670°C is in agreement with the X-ray strain in the TiC particles observed on figure 3.

The hydrostatic stress in the matrix, at the limit of the mesh is a tensile state, and it increases between 1100°C and 690°C. During the rapid transformation of the matrix, it decreases tending to a small compressive state, and increases for the lower temperatures reaching again a tensile state. Close to TiC particle, the stress evolution in the matrix at the "interface" is between that of TiC and that in the matrix at the limit of the mesh. The behaviour is strongly influenced by the TiC and follows an equivalent behaviour.

As temperature decreases, we can observe that due to the lower differences in CTE and the increase of mechanical properties of the matrix, no plastic deformation occurs between 670°C and 400ºC. Below this temperature, due to the particle interaction and evolution of the mechanical properties, we observe an increase of the Von Mises stress and plastic deformation. TiC particle is again in compression, as well as the matrix at the limit of the particle while the matrix at the limit of the mesh is in a tension.

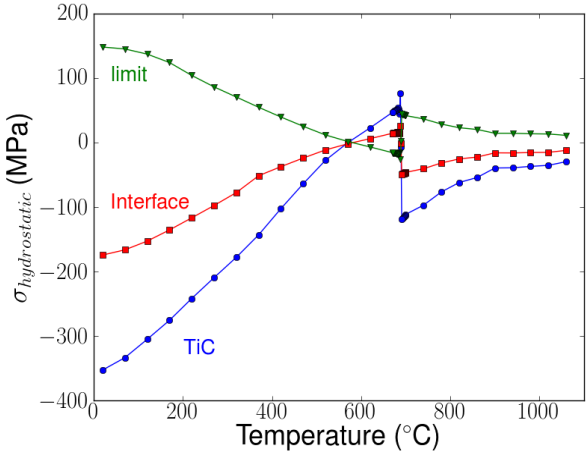

figure 6: Evolution of the hydrostatic stress versus temperature at different positions of the mesh.

We can note that the hydrostatic stress evolution in TiC particle and at the cell limit becomes non linear bellow about 400ºC. This evolution is in good agreement with the evolution of cell parameters and X-ray strain observed on figure 3.

6 Conclusions and perspectives

In situ X Ray structural characterizations of MMC were realized during a continuous thermal treatment involving a phase transformation of the matrix. The phase contents and the cell parameters evolutions of each phase were obtained. Development of stresses due to differences in CTE and phase transformations were evidenced.

A FE micromechanical model was used to calculate stresses generated during the cooling step. Evolutions of the calculated stresses are in good agreement with the evolutions observed by X-ray diffraction for the mean cell parameters and the X-ray strain in each phase, namely during the phase transformation and during cooling at the lower temperatures.

Additional calculations will be performed to take into account all the phases in the composite, to further analyse the interaction between the phases and to consider different transformations (i.e. martensitic transformation). Moreover, shape and particles size have also an influence on the final stress state; this point will be studied by using idealized particle with various shape and size and also with images from real microstructures.

In addition, experiments are scheduled to extract from X-ray diffraction the full stress tensor in the phases in order to further compare experiments and modelling.

7 Aknowledgements

The authors gratefully acknowledge Mecachrome for supplying the materials, the Direction Générale des Entreprises (DGE) for financial support in the AMETIS program, and the European Synchrotron Radiation Facility for provision of beamline ID15B.

References

[1] Akhtar F., Microstructure evolution and wear properties of in situ synthesized TiB2 and TiC reinforced steel matrix composites, *Journal of Alloys and Compound*, **459**, pp. 491-497 (2008).

[2] Pagounis E. & Lindroos V.K., Processing and properties of particulate reinforced steel matrix composites, *Materials Science and engineering A*, **246**, pp. 221-234 (1998)

[3] Pagounis E., Haimi E., Pietikäinen J., Talvitie M., Vahvaselkä S. & Lindroos V.K. , Effect of thermal expansion coefficients on the martensitic transformation in a steel matrix composite, *Scripta Materialia*, **34**, pp. 407-413 (1996)

[4] Geandier G., Hazotte A., Denis S., Mocellin A. & Maire E., Microstructural analysis of alumina chromium composite by X-Ray tomography and 3-D finite element simulation of thermal stresses, *Scripta Materialia*, **48**, pp. 1219-1224 (2003)

[5] Mourot M., Courleux A., Dehmas M., Gautier E., Geandier G., Dezellus O., Viala J. C., Martin O., Karnatak N. & Danoix F., Transformation Kinetics and Resulting Microstructure in MMC Reinforced with TiC Particles, *Solid State Phenomena*, **172-174**, pp. 747-752 (2011)

[6] Lee R., Chen G. & Hang B., Thermal and grinding induced residual stresses in a silicon carbide particle-reinforced aluminium metal matrix composites, *Composites*, **26**, pp. 425-429 (1995)

[7] Meixner M., Fitzpatrick M. & Reimers W. Measurement of the evolution of internal strain and load partitioning in magnesium hybrid composites under compression load using in-situ synchrotron X-ray diffraction analysis, *Composites Science and Technology*, **71**, pp. 167-176 (2011)

[8] Denis S., Archambault P., Gautier E., Simon A. & Beck G., Prediction of residual stresses and distortion of ferrous and non-ferrous metals: current status and future developments, *Journal of Materials Engineering and Performance*, **11** (1) pp. 92-102 (2002)
[9] Zheng Y., Cui L., Zhu D. & Yang D., The constrained phase transformation of prestrained TiNi fibers embedded in metal matrix smart composite, *Materials Letters*, **43**, pp. 91-96 (2000)
[10] Zwigl P. & Dunand D. C. Transformation Superplasticity of Iron and Fe/TiC Metal Matrix Composites, *Metallurgical and Materials Transactions A*, **29A**, pp. 565-575 (1998)
[11] Hammersley A. P., Svensson S. O., Hanfland M., Fitch A N & Häusermann D., Two-dimensional detector software: From real detector to idealised image or two-theta scan , *high pressure research*, **14**, pp.235-248 (1996)
[12] Rietveld H. M., A Profile Refinement Method for Nuclear and Magnetic Structures, *Journal of Applied Crystallography*, **2**, pp. 65-71 (1969)
[13] Rodríguez-Carvajal J., Recent advances in magnetic structure determination by neutron powder diffraction , *Physica B: Condensed Matter*, **192**, pp. 55-69 (1993)
[14] http://www.mat.ensmp.fr/index.php/Competences/ZeBuLoN/
[15] Denis S., Archambault P. & Gautier E., Models for stress-phase transformation couplings in metallic alloys, Academic Press, pp. 896-904 (2001)
[16] Ganghoffer J.F., Denis S., Gautier E., Simon A., Sjöström S., Finite element calculation of the micromechanics of a diffusional transformation, *European Journal of Mechanics A/Solids* **12**, pp 21-32 (1993).
[17] Gautier E., Denis S., Liebaut Ch., Sjöström S., Simon A., Mechanical behaviour of Fe-C alloys during phase transformations, *Journal de Physique IV, Colloque C3* **4,** pp 279-284 (1994).
[18] Wall J., Choo H., Tiegs T. N. & Liaw P. K., Thermal residual stress evolution in a TiC–50 vol.% Ni3Al cermet, *Materials Science and Engineering A*, **421**, pp. 40–45 (2006)